

# CHAMP & TIE-GCM MAGNETIC PERTURBATION COMPARISONS

David T. Mozzoni<sup>(1),(3)</sup>, M. Manda<sup>(1)</sup>, and J. C. Cain<sup>(2)</sup>

<sup>(1)</sup>*GeoForschungsZentrum Potsdam, Telegraphenberg, 14473 Potsdam, GERMANY, dmozzoni@gfz-potsdam.de, mioara@gfz-potsdam.de*

<sup>(2)</sup>*Geophysical Fluid Dynamics Institute, Florida State University, Tallahassee, FL 32306-4360 USA, cain@gfdi.fsu.edu*

<sup>(3)</sup>*Department of Physics, Florida State University, Tallahassee, FL 32306-4360 USA*

## ABSTRACT

The NCAR Thermosphere-Ionosphere Electrodynamic General Circulation Model (TIE-GCM) is a self-consistent global atmospheric model which can be used to estimate magnetic perturbations at satellite altitude. These computed perturbations can then be compared with CHAMP satellite magnetic vector data.

In this initial study, only the quietest day of each month was selected for this comparison. CHAMP magnetic vector residuals were then computed for these intervals using the CHAOS model to remove the core and crustal geomagnetic contributions. Under various input parameters, the TIE-GCM predictions were then computed and compared with the CHAMP residuals on an orbit by orbit basis.

Initial results demonstrate a reasonable agreement between the TIE-GCM estimates and the CHAMP residuals especially in non-polar regions ( $\pm 50^\circ$  Latitude) where both are able to resolve the Equatorial Electro-Jet (EEJ) and Solar Quiet (Sq) current systems.

## 1. INTRODUCTION

The present study is an initial effort to better understand the external sources of the magnetic field hoping that it may in turn help with the development of future geomagnetic models. The Thermosphere-Ionosphere Electrodynamic General Circulation Model (TIE-GCM) [3] is a self-consistent global atmospheric model being developed at the National Center for Atmospheric Research (NCAR) in Boulder, Colorado. This model can be used to predict many different atmospheric quantities, such as wind velocities, various atmospheric species concentrations, temperatures, electric fields, and current densities. The current densities can later be post-processed to compute magnetic perturbations both above and below the ionosphere. In order to validate these model results, one can compare the predicted perturbations calculated at the altitude of the CHAMP satellite (taken to be 430km) with vector residuals computed from the difference of the

CHAMP data and the CHAOS geomagnetic model [2]. For the first comparison, the quietest day of each month from 2001 – 2003 according to the list of international Q-days, was selected (see Sec. 7 for a list of websites). New residuals can then be computed between the original CHAMP/CHAOS residuals and estimates from the different TIE-GCM model runs for these quiet days.

### 1.1. CHAMP

The Challenging Minisatellite Payload (CHAMP) is a low Earth orbiting German satellite managed by GeoForschungsZentrum-Potsdam. Since its launch on July 15, 2000, this multi-mission satellite has supplied high precision, invaluable magnetic, gravity, and ion drift measurements. The geomagnetic field measurements, nearly six years worth, coupled with the other orbiting missions have allowed for the development of global field models of the core and its secular variation with unprecedented resolutions. Recent examples would include main field models like CHAOS [2], and static lithospheric field models such as MF4 [1].

### 1.2. CHAOS

The CHAMP, Ørsted and SAC-C (CHAOS) [2] model describes the Earth's magnetic field over the last few years. It models the geomagnetic field using spherical harmonics up to degree  $n = 50$  for the static field,  $n = 18$  for the first time derivative (secular variation), and  $n = 14$  for the quadratic and cubic time derivatives. It was developed using geomagnetic measurements from Ørsted, CHAMP and SAC-C taken between 03/1999 – 12/2005, spanning over 6.5 years of high-precision geomagnetic satellite data. It incorporates into its dataset higher than usual geomagnetic activity ( $K_p \leq 2$ ). Temporal variation of the core field is described by splines (for  $n \leq 14$ ). It uses magnetometer vector data in the instrument frame and co-estimates the Euler angles that describe the transformation from the magnetometer frame to the star imager frame, thus avoiding the inconsistency of using vector data that have been aligned using a different (pre-

existing) field model. The bending of the CHAMP optical bench, connecting the magnetometer and star imager, is taken into account by estimating Euler angles in 10 day segments. It also co-estimates  $n = 1$  external fields separately for every 12 hour interval.

### 1.3. TIE-GCM

The TIE-GCM [3] is a self-consistent simulation of neutral winds, conductivities, electric fields, various atmospheric species concentrations, and current densities. Below  $60^\circ$  magnetic latitude the electric field is calculated by solving for the dynamo equation, while above that the electric field is imposed. It uses the International Geomagnetic Reference Field (IGRF) with modified magnetic apex coordinates [4]. Geomagnetic field lines are assumed to be equipotential, which reduces the electrodynamic equation to two dimensions. Field-aligned current flows between hemispheres so that the divergence of the total current vanishes. Induced Earth currents are simulated assuming a perfectly conducting layer at a depth of  $600km$  below the Earth's surface. Height-integrated horizontal ionospheric currents are treated as currents in a thin shell at an altitude of  $110km$ , connected to field-aligned currents.

### 1.4. Calculation of Magnetic Perturbations

The calculation process for magnetic perturbations involves making a few assumptions [5]. Height-integrated horizontal ionospheric currents are treated as currents in a thin shell located at an altitude of  $110km$ , and connected to field-aligned currents. The field-aligned currents are treated as flowing on dipolar field lines, while zonal currents in the magnetosphere are ignored. Induced Earth currents are simulated by a perfectly conducting layer at a depth of  $600km$  below the surface of the Earth. Calculated ground magnetic effects are used to define equivalent horizontal ionospheric currents in a shell at a height of  $110km$ .

From the TIE-GCM, a thin shell of height-integrated horizontal ionospheric current density is produced. The equivalent current system, a fictitious divergence-free current sheet which produces the same magnetic perturbations at the ground, is then calculated. The equivalent current function can be expressed as an expansion in spherical harmonic coefficients which are then used to calculate the magnetic potential. From the magnetic potential one can compute the magnetic field perturbations.

## 2. DATES SELECTED FOR INVESTIGATION

In order to minimize magnetospheric and other transient effects, it was decided to use only days with low geomagnetic activity for this initial comparison study (this will

Table 1. The selected dates used in this comparison study represent the quietest day of each month from 2001 – 2003 as determined by the list of International Q-days.

Date (2001)	Date (2002)	Date (2003)
Jan 01, 2001	Jan 03, 2002	Jan 09, 2003
Feb 03, 2001	Feb 14, 2002	Feb 25, 2003
Mar 15, 2001	Mar 17, 2002	Mar 25, 2003
Apr 30, 2001	Apr 08, 2002	Apr 07, 2003
May 31, 2001	May 24, 2002	May 04, 2003
Jun 28, 2001	Jun 28, 2002	Jun 12, 2003
Jul 28, 2001	Jul 14, 2002	Jul 08, 2003
Aug 16, 2001	Aug 06, 2002	Aug 31, 2003
Sep 10, 2001	Sep 23, 2002	Sep 28, 2003
Oct 24, 2001	Oct 13, 2002	Oct 11, 2003
Nov 03, 2001	Nov 08, 2002	Nov 28, 2003
Dec 09, 2001	Dec 18, 2002	Dec 19, 2003

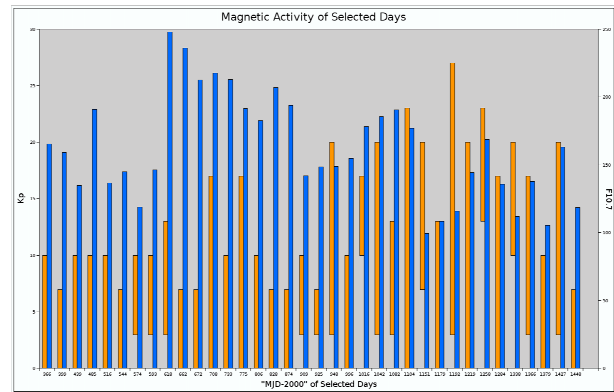


Figure 1. Some of the activity indices  $K_p$  range (Orange) and  $F10.7$  (Blue) for the selected dates used in this comparison study.

be relaxed in future studies). The selected dates represent the quietest day of each month, in terms of geomagnetic activity, from 2001 – 2003 as determined by the list of International Q-days. Tab. 1 details the actual dates investigated while their corresponding magnetic activity is displayed in Fig. 1.

## 3. TIE-GCM METHOD & RESULTS

The TIE-GCM was used to model each of the quiet days listed in Tab. 1. In order to investigate its sensitivity, the following five cases of the input  $F10.7$  were used for each day:  $F10.7 = 70$ ,  $F10.7 = 90$ ,  $F10.7 = 150$ ,  $F10.7 = 190$ , and  $F10.7 = GPI$  (uses real-time values interpolating for every time-step (2 minutes)).

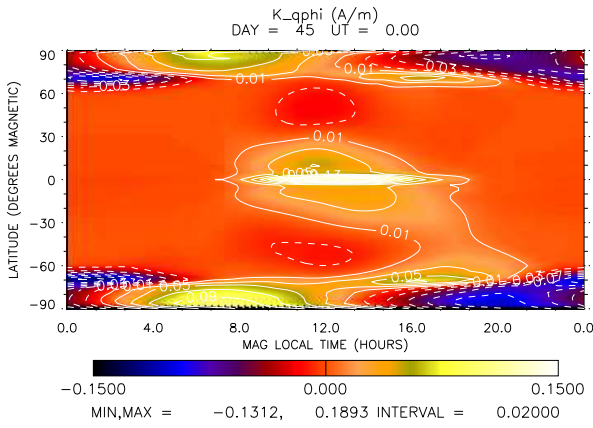


Figure 2. The Eastward component of the Height-Integrated Horizontal Current Density predicted by the TIE-GCM for February 14, 2002 using GPI inputs.

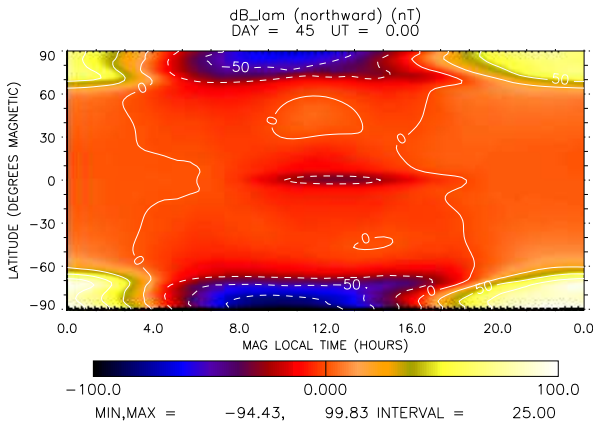


Figure 3. The Northward component of the magnetic perturbation predicted by the TIE-GCM for February 14, 2002 using GPI inputs.

Fig. 2 represents the TIE-GCM prediction of the Height-Integrated Horizontal Current Density for February 14, 2002 using real-time GPI inputs rather than fixed activity index values for the Eastward component. The EEJ signature has been reproduced in the Eastward component, with an amplitude of around  $0.15 A/m$ .

Fig. 3 represents the Northward component at satellite altitude of the magnetic perturbation, produced by post-processing the TIE-GCM predictions of current densities, for February 14, 2002 using real-time GPI inputs. The EEJ signature seen in the Eastward component of the height-integrated current density produces a negative magnetic perturbation, of order  $-30 nT$ , in the Northward magnetic perturbation component.

#### 4. COMPARISON OF MODEL RESULTS

The TIE-GCM magnetic perturbation predictions (Fig. 3) were compared to the CHAMP-CHAOS residuals along the orbit-track in order to produce Fig. 4. The full CHAOS model was used to compute residuals for the corresponding CHAMP vector measurements. Also plotted is a curve representing the residual calculated from the difference of the CHAMP/CHAOS residual and the predicted TIE-GCM magnetic perturbation. The CHAMP/CHAOS and CHAMP/CHAOS/TIE-GCM residuals have had their mean subtracted so as to remove their offset from zero and bring all datasets to a common level. The CHAMP satellite was in approximately a 10 solar local time (SLT) plane. In the top and bottom left-hand corners, are displayed the absolute mean deviation, mean and area under the curve in the following format:  $[MDEV(MEAN) - AREA]$ .

The EEJ signature seen in  $B_\theta$  (Fig. 4(c)) for this particular orbit pass is fairly well reproduced in location, even though the amplitude is quite a bit smaller. This component yields both a smaller MDEV (spread) and Mean (offset), likewise for the total field (Fig. 4(a)). In this case the run with the  $F_{10.7}$  held fixed at 190 seems to have produced the best overall fit (the actual  $F_{10.7}$  for this date was 191.3).

The plot window for the  $B_r$  component (Fig. 4(b)) shows the ability of the TIE-GCM to reproduce the low/high transition centered around the magnetic equator associated with Sq, however its poorer job in the tail region has it netting a worse overall MDEV and Mean. The  $B_\phi$  component (Fig. 4(b)) shows a mixed result whereby the model matched a slight trend but the amplitude was off causing a better MDEV but worse Mean.

#### 5. SUMMARY OF RESULTS

Fig. 5 actually represents a relatively good fit, whereas many individual day comparisons show more inconsistent results. In Fig. 5(a) the TIE-GCM models generally show an improvement by reducing the MDEV and Mean for the  $B_\theta$  component. Though not displayed, the total field  $B_F$  shows a similar character. As is typical, the  $B_r$  (Fig. 5(b)) and  $B_\phi$  (not shown) components are more inconsistent, varying from having a positive influence to having a negative influence over the course of the day.

It is hard to draw anything conclusive, Fig. 6 is just an average for one day during the month after all, but overall the TIE-GCM models seem to help more than they hurt. For instance, the 2003 MDEV Average for  $B_\theta$  is consistently lower than the data alone, save for the month of August.

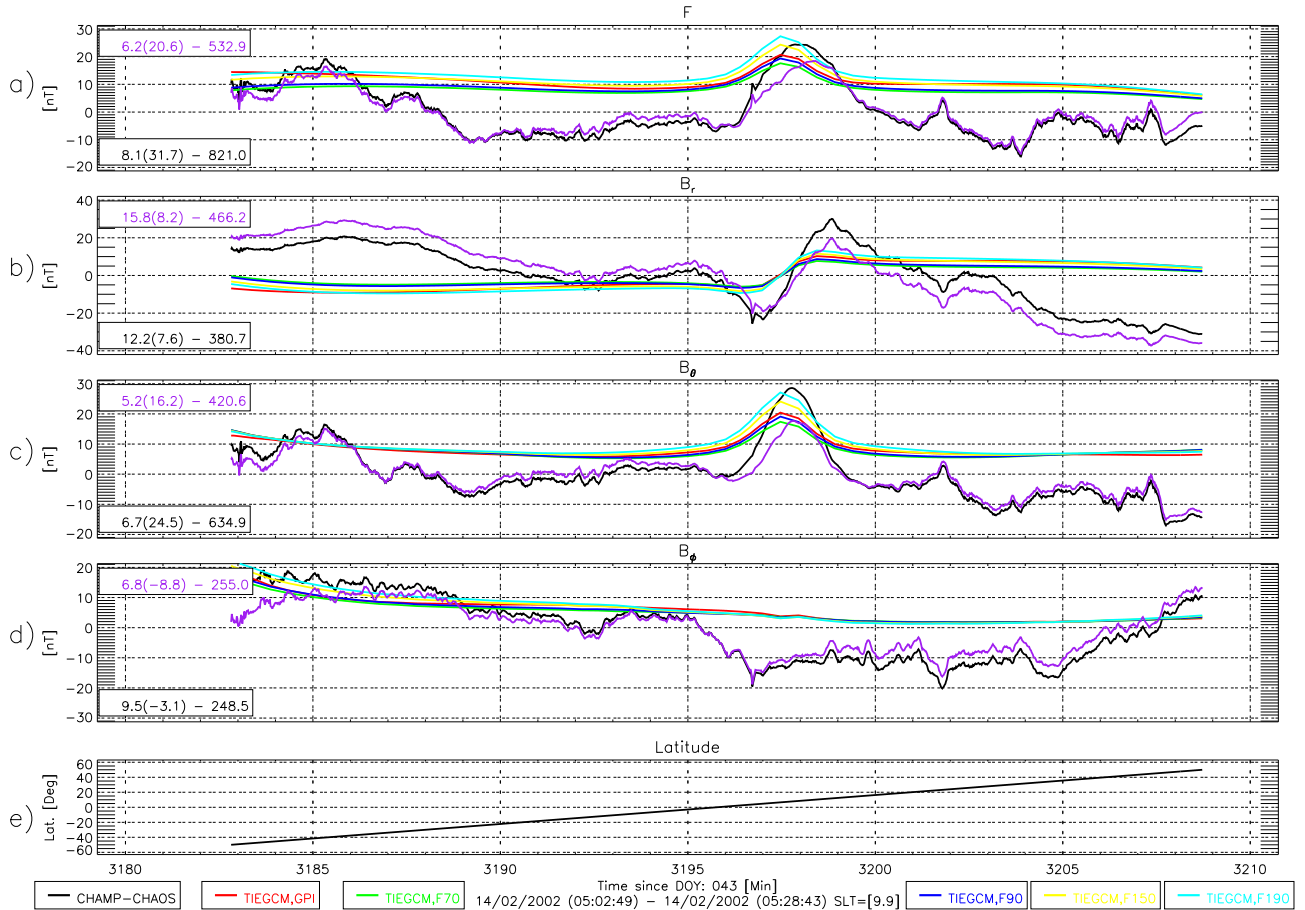


Figure 4. This plot displays the residual and TIE-GCM perturbation prediction data along the satellite orbit track for one orbit pass on February 14, 2002 between  $\pm 50^\circ$  latitude. The plot windows correspond to (a) the total field perturbation, (b) the  $B_r$  component of the perturbation, (c) the  $B_\theta$  component, (d) the  $B_\phi$  component, and (e) the satellite latitude. All five TIE-GCM model runs are shown vs. the CHAMP data and perturbation residuals using the following color scheme:  $F_{10.7} = 70$  (Green),  $F_{10.7} = 90$  (Blue),  $F_{10.7} = 150$  (Yellow),  $F_{10.7} = 190$  (Cyan),  $F_{10.7} = \text{GPI}$  (Red), CHAMP/CHAOS Residual (Black), and CHAMP/CHAOS/TIE-GCM(GPI) Residual (Purple).

## 6. CONCLUSIONS

For this study, the TIE-GCM was used to simulate the magnetic perturbations at CHAMP satellite altitude during the lowest geomagnetically active days of each month from 2001 – 2003. For each of these days the modeling was carried out using five different cases of the input parameter  $F_{10.7}$ . The model results were then compared with residuals of vector geomagnetic field measurements computed from the difference of CHAMP data and the CHAOS geomagnetic field model.

From the above plots in this initial study, one can see that the TIE-GCM can, to some degree, reproduce the residuals computed from CHAMP geomagnetic vector data. However the quality of the comparison is rather inconsistent, sometimes helpful and sometimes not. This is evidenced in the Mean average of the  $B_\theta$  component for 2003 (Fig. 6), where there is a marked improvement from May until September, but an equally marked worsening

for the other months. For that same component however, the MDEV is consistently better for the years 2002 and 2001, but not in  $B_F$ .

But overall, the fact that a model derived using no *in-situ* magnetic data can match features in satellite data at all is promising. This modeling approach better lends itself to an understanding of the physics of the ionospheric sources than would a purely parameterized model.

Clearly further study is needed to better pin-down under what conditions the model best predicts the data. To proceed in this direction it is important to expand the tested parameter space to include inputs other than just  $F_{10.7}$ . These would include varying TIE-GCM inputs like the cross-tail potential, the hemispheric power, the atmospheric tides, and the electric potential model. Also broadening the selection criteria to include alternative methods of data selection like those based on the wavelet power spectrum [6], or conversely to purposely include days with more elevated geomagnetic activity,

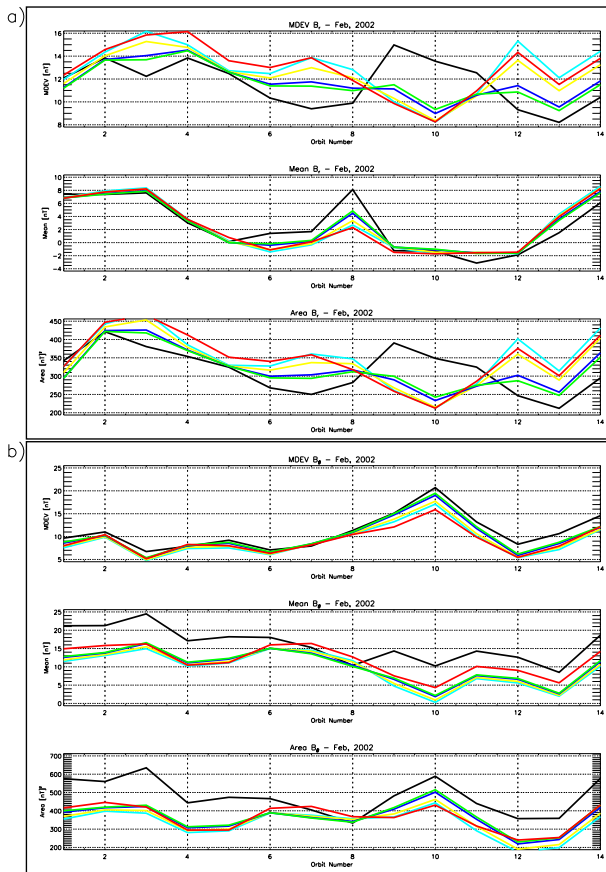


Figure 5. These plots show the statistics of the dayside orbit passes for February 14, 2002: MDEV (top), Mean (middle), and Area (bottom). The CHAMP/CHAOS/TIE-GCM  $B_r$  (a) and  $B_\theta$  (b) residuals from Fig. 4 are shown vs. the orbit number. All five TIE-GCM model runs (GPI (Red),  $F_{10.7} = 70$  (Green),  $F_{10.7} = 90$  (Blue),  $F_{10.7} = 150$  (Yellow),  $F_{10.7} = 190$  (Cyan)) and the CHAMP residuals (Black) are displayed.

should prove informative. A thorough investigation of the dependence on solar cycle and season also needs to be addressed. A more robust way of quantifying the quality of fit also needs to be developed as the current method of using the MDEV and Mean statistics are insufficient and can occasionally be slightly misleading for individual tracks.

## 7. WEBSITES

- CHAMP Satellite  
[www.gfz-potsdam.de/pb1/op/champ](http://www.gfz-potsdam.de/pb1/op/champ)
- CHAOS Geomagnetic Model  
[www.gfz-potsdam.de/pb2/pb23/Models/CHAOS](http://www.gfz-potsdam.de/pb2/pb23/Models/CHAOS)
- International Q-days  
[www.gfz-potsdam.de/pb2/pb23/GeoMag/niemegk/kp\\_index/quietdst](http://www.gfz-potsdam.de/pb2/pb23/GeoMag/niemegk/kp_index/quietdst)

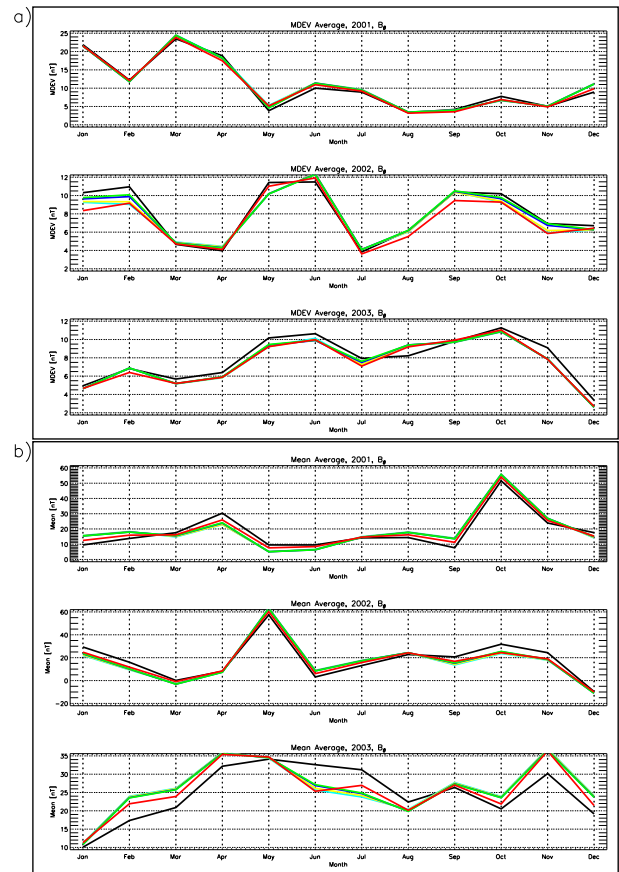


Figure 6. These plots show the time-series of the average orbit pass statistics MDEV (a) and Mean (b) (nT vs. Month) for each of the selected days spanning the years 2001 (top), 2000 (middle), and 2003 (bottom) for the  $B_\theta$  component. All five TIE-GCM model runs are represented (GPI (Red),  $F_{10.7} = 70$  (Green),  $F_{10.7} = 90$  (Blue),  $F_{10.7} = 150$  (Yellow),  $F_{10.7} = 190$  (Cyan)) as well as the CHAMP residuals (Black).

- $K_p$  &  $F_{10.7}$  Magnetic Indices  
[www.gfz-potsdam.de/pb2/pb23/GeoMag/niemegk/kp\\_index](http://www.gfz-potsdam.de/pb2/pb23/GeoMag/niemegk/kp_index)
- TIE-GCM  
[web.hao.ucar.edu/public/research/iso/tgcm/tgcm.html](http://web.hao.ucar.edu/public/research/iso/tgcm/tgcm.html)

## REFERENCES

- [1] Maus, S., M. Rother, K. Hemant, H. Lühr, A. Kuvshinov, and N. Olsen, Earth's lithospheric magnetic field determined to spherical harmonic degree 90 from CHAMP satellite measurements *Geophys. J. Int.*, 164, 319–330, doi: 10.1111/j.1365-246X.2005.02833.x, 2006.
- [2] Olsen, N., H. Lühr, T. J. Sabaka, M. Manda, M. Rother, L. Tøffner-Clausen, and S. Choi, CHAOS – A Model of Earth's Magnetic Field derived from

CHAMP, Ørsted, and SAC-C magnetic satellite data, *Geophys. J. Int.*, in press, 2006.

- [3] Richmond, A. D., E. C. Ridley, and R. G. Roble, A Thermosphere/Ionosphere General Circulation Model with Coupled Electrodynamics, *Geophys. Res. Lett.*, 19, 601–604, 1992.
- [4] Richmond, A. D., Ionospheric electrodynamics using magnetic apex coordinates, *J. Geomag. Geoelectr.*, 47, 191–212, 1995.
- [5] Richmond, A. D., Modeling the geomagnetic perturbations produced by ionospheric currents, above and below the ionosphere, *J. Geodyn.*, 33, 143–156, 2002.
- [6] Schachtschneider, R., G. Balasis, M. Rother, M. Manda, Wavelet-based selection of satellite data for geomagnetic field modelling, First Swarm International Science Meeting, Proceedings, May 3–5, 2006.